

# Long range optical phonons in liquid water

D. C. Elton<sup>1</sup> and M.-V. Fernández-Serra<sup>1,2</sup>

<sup>1)</sup>Department of Physics and Astronomy, Stony Brook University, Stony Brook, New York 11794-3800, USA

<sup>2)</sup>Institute for Advanced Computational Sciences, Stony Brook University, Stony Brook, New York 11794-3800, USA

In this work we show that on subpicosecond time scales optical phonon modes can propagate through the H-bond network of water over distances of up to two nanometers. Using molecular dynamics simulation we find propagating optical phonons in the librational and OH stretching modes. Both of these phonons exhibit longitudinal-transverse splitting at  $k = 0$ , indicating the presence of long range dipole-dipole interaction. Since such splitting is intimately connected to structure, our analysis opens the door for new insights into how the structure of water changes with temperature. Our results also explain a previously unnoticed discrepancy one encounters when comparing the librational peaks found in Raman spectra with those in infrared and dielectric spectra. Previously the three librational peaks in Raman spectra were assigned to the librations of single molecules. Our results indicate these peaks are better understood as a transverse phonon, the wagging libration, and a longitudinal phonon.

The local structure of water as a function of temperature remains a source of intense research and lively debate.<sup>1–5</sup> In this work we show how the dielectric susceptibility can be used as a novel probe of the local structure of the liquid. From existing dielectric data it is easy to show that some of the optical modes of water exhibit longitudinal-transverse (LO-TO) splitting. In the limit of infinite wavelength ( $k \rightarrow 0$ ) the longitudinal and transverse dielectric susceptibilities can be obtained from the dielectric function via the following relations:<sup>6,7</sup>

$$\chi_L(k \rightarrow 0, \omega) = 1 - \frac{1}{\varepsilon(\omega)} \quad (1)$$

$$\chi_T(k \rightarrow 0, \omega) = \varepsilon(\omega) - 1 \quad (2)$$

Note that the transverse susceptibility is what one normally calls “susceptibility”. The dielectric function can be obtained from the index of refraction  $n(\omega)$  and extinction coefficient  $k(\omega)$  as:

$$\begin{aligned} \varepsilon'(\omega) &= n^2(\omega) - k^2(\omega) \\ \varepsilon''(\omega) &= 2n(\omega)k(\omega) \end{aligned} \quad (3)$$

These equations allow us to use previously published data<sup>8,9</sup> to calculate the imaginary part of the longitudinal response. We find significant LO-TO splitting in the librational and stretching bands (fig. 8). LO-TO splitting indicates the presence of long-range dipole-dipole interactions in the system. It was previously shown that the librational peak in the longitudinal dielectric susceptibility of water is dispersive,<sup>10</sup> and Bopp, et. al. noted that the dispersion relation has the appearance of an optical phonon mode.<sup>11</sup> We show that the transverse counterpart also exhibits such dispersion and argue that the dispersive modes in the dielectric susceptibility are due to optical phonons which travel along the H-bond network of water.

Our work solves a thus far unrecognised discrepancy that exists between the peak assignments reported in

studies of the Raman and dielectric/IR spectra of water. Although early experimentalists fit the Raman librational band with two peaks,<sup>12,13</sup> it is better fit with three (see Supplementary Table 1).<sup>14–18</sup> Previously these three peaks were assigned to the three librational motions of the water molecule - “twisting” ( $\approx 435 \text{ cm}^{-1}$ ), “rocking” ( $\approx 600 \text{ cm}^{-1}$ ) and “wagging” ( $\approx 770 \text{ cm}^{-1}$ ).<sup>14,15,17</sup> However, when comparing these assignments to infrared and dielectric spectra, one runs into a serious discrepancy. One expects to find the two higher frequency peaks to be present, since only the rocking and wagging librations are IR active. The “twisting” libration, consisting of a rotation of the hydrogen atoms around the C2 axis, is not IR active since it does not affect the dipole moment of the molecule. Instead, IR spectra show two peaks at 380 and  $665 \text{ cm}^{-1}$ ,<sup>19</sup> and similarly dielectric spectra yield two peaks at 420 and  $620 \text{ cm}^{-1}$ ,<sup>20</sup> in disagreement with this assignment. Our results indicate that the lowest frequency Raman peak ( $\approx 435 \text{ cm}^{-1}$ ) is actually a transverse optical phonon mode while the highest frequency Raman peak ( $\approx 770 \text{ cm}^{-1}$ ) is a longitudinal optical phonon mode. This explains why the highest frequency Raman mode does not appear in IR or dielectric experiments, since they only probe the transverse response. This method of assigning Raman peaks is the same method that has been used to assign longitudinal phonon modes to the Raman spectra of ice Ih,<sup>21–23</sup> ice Ic,<sup>24</sup> and vitreous  $\text{GeO}_2$  and  $\text{SiO}_2$ .<sup>25</sup> We understand the remaining middle peak in the Raman spectra by studying how the single molecule response (the self part) is cancelled out by intermolecular correlations (the distinct part).

One way to understand LO-TO splitting is through the Lyddane-Sachs-Teller (LST) relation:<sup>26</sup>

$$\frac{\omega_{\text{LO}}^2}{\omega_{\text{TO}}^2} = \frac{\varepsilon(0)}{\varepsilon_\infty} \quad (4)$$

Although the LST relation was originally derived for a cubic ionic crystal it was later shown to have very general applicability,<sup>27,28</sup> and has been applied to disor-

dered and glassy solids.<sup>23,29,30</sup> To apply this equation to water we must use a generalized LST (gLST) relation which takes into account all of the optically active modes in the system and the effects of dampening.<sup>27</sup> The gLST relation reads as:<sup>27</sup>

$$\prod_i \frac{\omega_{LDi}}{\omega_{TDi}} \prod_j \frac{|\bar{\omega}_{Lj}|^2}{\omega_{Tj}^2} = \frac{\varepsilon(0)}{\varepsilon_\infty} \quad (5)$$

Here the index  $i$  runs over the Debye peaks in the system and the index  $j$  runs over the number of damped harmonic oscillator peaks. The longitudinal frequencies of the damped harmonic oscillators must be considered as complex numbers ( $\bar{\omega}_{Li} = \omega_{Li} + i\gamma_i$ ), where  $\gamma_i$  is the dampening factor.

As shown by Barker, the gLST equation can be understood purely from a macroscopic point of view,<sup>27</sup> so by itself it yields little insight into microscopic dynamics. LO-TO splitting can be understood from a microscopic standpoint via the equation:<sup>31,32</sup>

$$\omega_{Lk}^2 - \omega_{Tk}^2 = \frac{4\pi C}{3v} \left( \frac{\partial \mu}{\partial Q_k} \right)^2 \quad (6)$$

Here  $v$  is the volume per unit cell,  $Q_k$  is the normal coordinate of the mode, and  $C$  is a prefactor which depends on the type of lattice and the boundary conditions of the region being considered (for an infinite cubic lattice,  $C = 1$ ). Equation 6 shows that LO-TO splitting is intimately related to crystal structure, so analyzing the LO-TO splitting provides a means of probing structural changes in liquid water as a function of temperature. As an example of this, equation 6 was recently used to test ideas about the quasi-symmetry of room temperature ionic liquids.<sup>33</sup>

As in our last study<sup>34</sup> we compared results from a rigid (TIP4P/ $\varepsilon$ ) model, a flexible model (TIP4P/2005f), and a flexible and polarizable model (TTM3F) in all of our analyses.

## I. RESULTS

### A. Polarization correlation functions

The longitudinal and transverse polarization correlation functions at small  $k$  are shown in figure 1 for TIP4P/ $\varepsilon$ . Since TIP4P/ $\varepsilon$  is a rigid model, only librational motions are present. The addition of flexibility and polarizability add additional high frequency oscillations to the picture (see Supplementary Fig. 1). In the small wavenumber regime ( $k < 1.75\text{\AA}^{-1}$ ) there is a damped oscillation which corresponds to the collective librational phonon mode. This damped oscillation is superimposed on an underlying exponential relaxation in both the transverse and longitudinal cases. In the longitudinal case the underlying relaxation time  $\tau(k)$  of the exponential relaxation exhibits non-monotonic behaviour

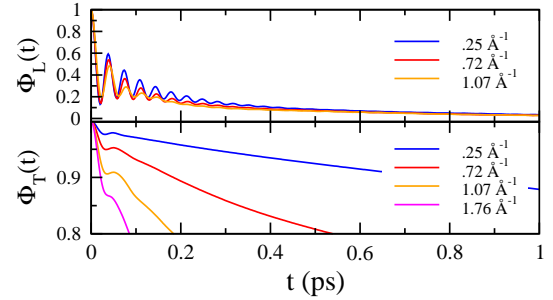


FIG. 1: **Polarization correlation functions for TIP4P/ $\varepsilon$ .** Longitudinal (top) and transverse (bottom) polarization correlation functions (equation 13). The oscillations at small  $k$  come from the collective librational mode, which is much more pronounced in the longitudinal case.

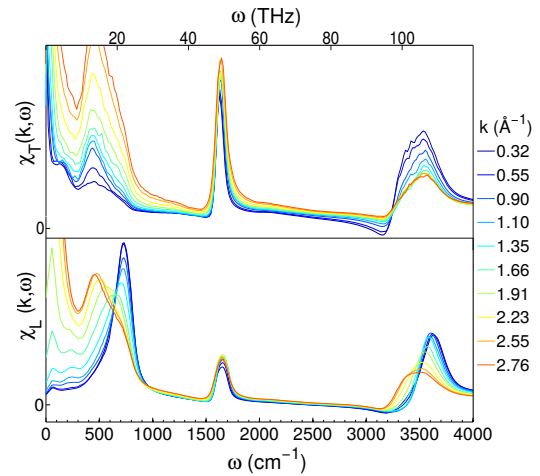


FIG. 2: **Imaginary part of the transverse (top) & longitudinal (bottom) susceptibility for TTM3F at 300 K.** Both the librational ( $\approx 750 \text{ cm}^{-1}$ ) and OH stretching peak ( $\approx 3500 \text{ cm}^{-1}$ ) exhibit dispersion in the longitudinal case.

with  $k$ , reaching a maxima at  $k \approx 3\text{\AA}^{-1}$  (see Supplementary Fig. 2). At wavenumbers greater than  $k \approx 2.5\text{\AA}^{-1}$  only intramolecular motions contribute to the relaxation. Intriguingly, close inspection of the longitudinal correlation function at small  $k$  shows that small-magnitude librational oscillations persist longer than one picosecond before eventually loosing coherence (see Supplementary Fig. 3).

### B. Dispersion of the librational peak

Figure 2 shows the imaginary part of the longitudinal and transverse susceptibility for TTM3F. In the longitudinal case the librational peak is clearly seen to shift with  $k$ . In the transverse case, the lower frequency portion of the band is seen to shift slightly with  $k$ . Dis-

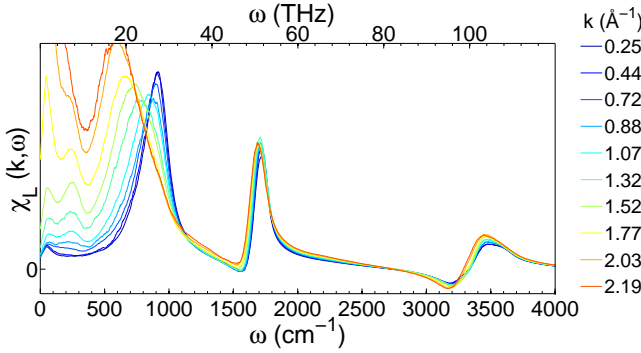


FIG. 3: **Imaginary part of the longitudinal susceptibility for TIP4P/2005f at 300 K.** No dispersion is observed in the OH stretching peak.

ersion relations for the longitudinal and transverse librational peaks are shown in figure 4 for three different temperatures, using one peak fits. The dispersion relations appear to be that of optical phonons. In both the longitudinal and transverse case the dampening factors remain less than the resonance frequencies, indicating an underdamped oscillation (see supplementary Fig. 4).

Resonance frequencies and lifetimes for the smallest  $k$  are shown in table ???. The speed of propagation of these modes was computed by finding the slope  $d\omega/dk$  in the regime of linear dispersion. For TIP4P/2005f we found speeds of  $\approx 2700$  m/s and  $\approx 1800$  m/s for the longitudinal and transverse modes. These propagation speeds are above the speed of sound in water (1500 m/s) but below the speed of sound in ice (4000 m/s). The temperature dependence of the propagation speed was found to be very small.

In both the longitudinal and transverse cases, the residual of the peak fitting shows features not captured by our Debye + one resonance fit of the librational peak. In both the longitudinal and transverse cases there is a non-dispersive peak at higher frequency, located at  $\approx 900$   $\text{cm}^{-1}$  for TIP4P/2005f and at  $\approx 650$   $\text{cm}^{-1}$  in TTM3F. This peak is negligibly small in the  $k = 0$  longitudinal susceptibility but appears as a shoulder as  $k$  increases. In the transverse case the overlapping peak persists at  $k = 0$ , so we found that the  $k = 0$  transverse spectra is best fit with two peaks, in agreement with experimental spectra. As we describe later, the higher frequency transverse peak is largely due to the self part of the response and is associated with the wagging librations of single molecules.

### C. Importance of polarizability

There are several notable differences between TTM3F and the non-polarizable model TIP4P/2005f. First of all, the librational band of TIP4P/2005f is at higher frequency, in worse agreement with experiment. More im-

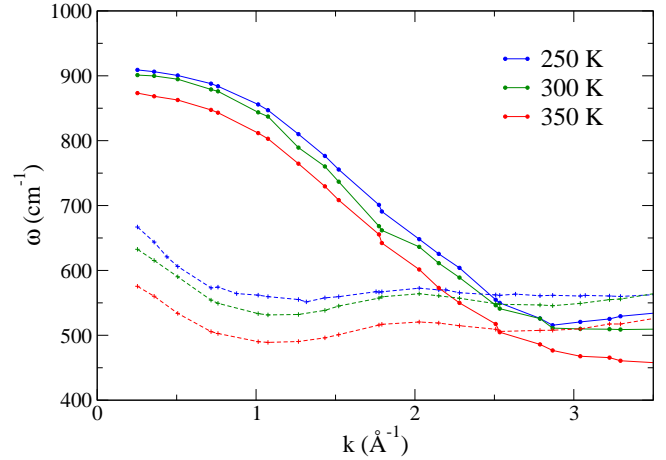


FIG. 4: **Dispersion relations for the propagating librational modes.** For TIP4P/2005f at three different temperatures (squares = longitudinal, pluses = transverse). A similar plot is found for TTM3F, but with lower frequencies.

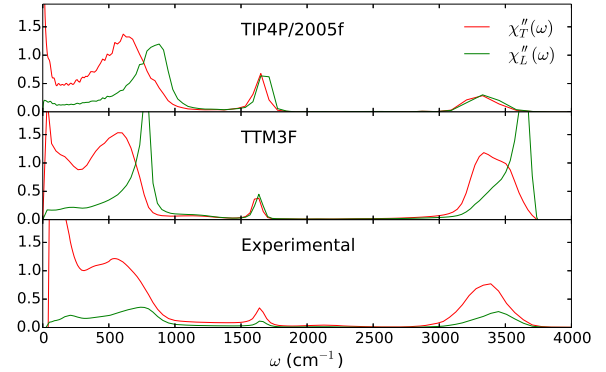


FIG. 5: **Imaginary parts of the transverse and longitudinal dielectric susceptibility.** We compare the non-polarizable model TIP4P/2005f, the polarizable model TTM3F, and experimental data<sup>9</sup> at 298 K. The effects of polarization can be seen in the LO-TO splitting of the stretching mode and in the low frequency features.

portantly, we find that TTM3F exhibits dispersion in the OH stretching band ( $\approx 3500$   $\text{cm}^{-1}$ ) in the longitudinal case while TIP4P/2005f does not. The transverse susceptibility of TTM3F does not exhibit such dispersion but the magnitude of the OH stretching band increases at small  $k$ , indicating long range intermolecular correlations. TIP4P/2005f does not exhibit this behavior. Similarly, at  $k = 0$  TTM3F exhibits significant LO-TO splitting in the OH stretching band while TIP4P/2005f does not (fig.5). These findings are consistent with Heyden's results for the  $k$ -resolved IR spectra from ab-initio simulation, where they concluded that polarization allows for intermolecular correlations at the OH-stretch

frequency.<sup>35</sup>

These findings can be understood from the dipole derivative in equation 6. In the librational band the derivative of the dipole moment with respect to normal coordinate is purely due to rotational-type motions. In the OH-stretching modes, on the other hand, the dipole derivative is due to changes in the geometry of the molecule and electronic polarization of the molecule during the OH stretching.<sup>1</sup> The dipole moment surface (fluctuating charges) and polarization dipole incorporated in TTM3F account for the changes in polarization that occur during OH stretching motion. These results confirm the significance of polarization in capturing the OH stretching response of water.<sup>35</sup>

Figure 5 shows a comparison of TTM3F, TIP4P/2005f and experiment at  $k = 0$ . While the location of the peaks in TTM3F are in good agreement with the experimental data at 298 K, the magnitude of the longitudinal response is greatly overestimated in TTM3F. The degree of LO-TO splitting in the OH stretching peak is also overestimated in TTM3F. In general it appears that TTM3F overestimates the dipole derivative in equation 6 while TIP4P/2005f underestimates it. Figure 5 also shows the effect of polarization at low frequencies, in particular the appearance of an H-bond stretching response at  $\approx 250$   $\text{cm}^{-1}$  in TTM3F which is absent in TIP4P/2005f.<sup>34</sup>

#### D. LO-TO splitting vs temperature

The frequencies of the librational and stretching modes are shown in table ???. Once again we compare our results to experimental data.<sup>8,9,37</sup> The comparison is imperfect since the TIP4P/2005f and TTM3F data comes from data at finite  $k$  (the smallest  $k$  in the system). For all three systems (TIP4P/2005f, TTM3F, and experiment) the increase in the LO-TO splitting of the librational band is puzzling, since the right hand side of the LST relation predicts a decrease in splitting, corresponding to a smaller dielectric constant and weaker dipole-dipole interactions. We found verifying the gLST equation is difficult because water contains either two or three Debye relaxations which must be taken into account.<sup>38,39</sup> Uncertainties in how to fit the region of 1 - 300  $\text{cm}^{-1}$  (.2 - 9 THz, which includes the contribution from many H-bonding modes, precludes a direct application of the gLST relation to water. By ignoring this region, however, we were able to achieve an approximate validation of the gLST equation for TIP4P/2005f (see Supplementary Information). A more detailed analysis of how to fit the low frequency region will be the focus of future work. Since the gLST equation is an exact sum rule it

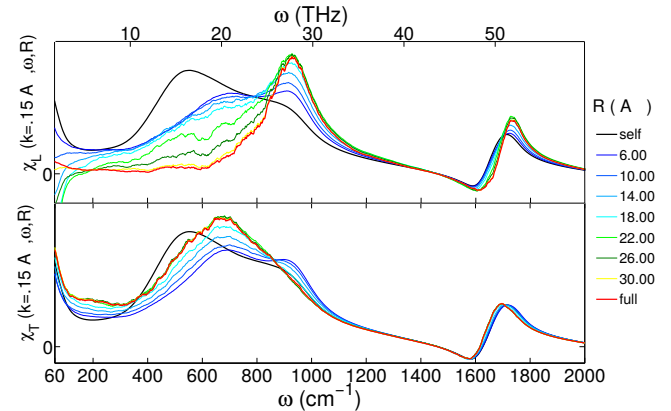


FIG. 6: **Imaginary part of the distance decomposed susceptibility for TIP4P/2005f.**

Longitudinal (top) and transverse (bottom) susceptibilities, calculated with a 4 nm box 300K, using the smallest  $k$  vector in the system. Gaussian smoothing was applied. Long range contributions to the librational peak extending to  $R = 2$  nm are observed.

can be used to assist in testing the validity of different fit functions.

#### E. Relation to phonons in ice

Naturally we would like to find corresponding optical phonon modes in ice. As shown in figure 8 the infrared spectra and LO-TO splitting of supercooled water resembles that of ice. Recently evidence has been presented for propagating librational phonon modes in ice XI.<sup>40,41</sup> Three of the twelve librational modes of ice XI are IR active (labeled WR1, RW1 and RW2) and all three exhibit LO-TO splitting. The splittings have been found from Raman scattering to be 255, 135 and 35  $\text{cm}^{-1}$ .<sup>41</sup> These modes all consist of coupled wagging and rocking motions. The WR1 mode, which has the largest infrared intensity, most closely matches our results. WR1 and RW2 have the same transverse frequency and RW1 has a smaller infrared intensity, which may help explain why the librational band is well fit by a single optical mode. LO-TO splitting in the OH-stretching modes of ice Ih has been discussed previously.<sup>23</sup>

#### F. Range of propagation

The range of propagation of these modes can be calculated as  $R = \tau v_g$  where  $\tau$  is the lifetime and  $v_g = d\omega/dk$  is the group velocity. For TIP4P/2005f we find a range of propagation of  $\approx 1.1$  nm for the longitudinal librational mode and  $\approx .3$  nm for the transverse mode. Similar results hold for TTM3F.

To verify that the modes we observe are actually propagating and to further quantify the range of propagation

<sup>1</sup> In principle there may also be coupling between the librational and stretching motions, but typically such rotational-vibrational coupling effects are negligibly small.<sup>36</sup>

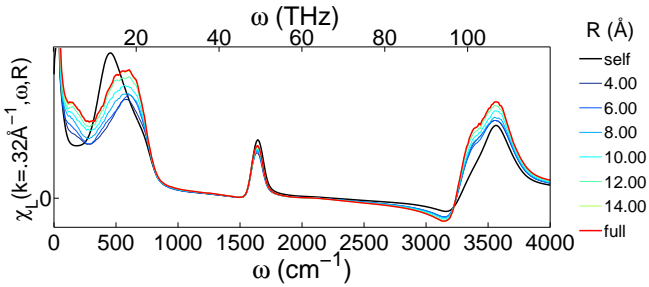


FIG. 7: **Imaginary part of the distance decomposed longitudinal susceptibility for TTM3F at 300 K.** Long range contributions are observed in the OH stretching band

we study the spatial extent of polarization dipole correlations as a function of frequency. We investigated several different methodologies that can be used to decompose a spectra into distance-dependent components (see Supplementary Information). We choose to start with the polarization correlation function:

$$\phi(k, t) = \left\langle \sum_i \mathbf{p}_i(k, 0) \cdot \sum_j \mathbf{p}_j(k, t) \right\rangle \quad (7)$$

Here  $\mathbf{k}, \mathbf{p}_i$  represents either the longitudinal or transverse molecular polarization vector of molecule  $i$ . We now limit the molecules in the second sum to those in a sphere of radius  $R$  around each molecule  $i$ :

$$\phi(k, t, R) = \left\langle \sum_i \mathbf{p}_i(k, 0) \cdot \sum_{j \in R_i} \mathbf{p}_j(k, t) \right\rangle \quad (8)$$

The resulting function exhibits the expected  $R \rightarrow 0$  limit, yielding only the self contribution. In the  $R \rightarrow \sqrt{3}L/2$  limit, the full response function for the simulation box is recovered. As  $R$  increases, the contributions of the distinct term add constructively and destructively to the self term, illustrating the contributions from molecules at different distances.

Figure 6 shows the distance decomposed longitudinal and transverse susceptibilities for TIP4P/2005f in a 4 nm box at the smallest  $k$  available in the system. The entire region between 0 - 1000 cm<sup>-1</sup> contains significant cancellation between the self and distinct parts, in qualitative agreement with a previous study.<sup>42</sup> In the longitudinal susceptibility, the self component has two peaks (at 500 and 900 cm<sup>-1</sup> for TIP4P/2005f) representing the two IR active librational motions (rocking and wagging, respectively). The self part is the same in both the longitudinal and transverse cases, reflecting an underlying isotropy which is only broken when dipole-dipole correlations are introduced. Further insight into the self-distinct cancellation comes from the results of Bopp, et. al., who project the hydrogen currents into a local molecular frame, allowing them to study the cross correlations between the rocking and wagging librations.<sup>11</sup> They find that in the

longitudinal case cross correlations between rocking and wagging contribute negatively in the region of 480 cm<sup>-1</sup> and positively in the region of 740 cm<sup>-1</sup>, suppressing the lower frequency peak to zero and enhancing the higher frequency peak.

In both the transverse and longitudinal cases as  $R$  increases a new peak emerges, corresponding to the propagating mode. The shift in the peak between the self and distinct parts rules out the possibility that the propagating mode is the controversial dipolar plasmon resonance since the dipolar plasmon must be a resonance of both the of single molecule and collective motion.<sup>43-45</sup> Interestingly, there are very long range contributions to this peak. In our simulations with a 4 nm box of TIP4P/2005f contributions persist up to 3 nm in the longitudinal case and 2 nm in the transverse case. As noted, recent studies of ice suggest that the propagating modes consist of coupled wagging and rocking librations.<sup>40,41</sup> The results for the transverse mode confirm this hypothesis, since the propagating mode peak lies between the single molecule rocking and wagging peaks. In the longitudinal case the propagating mode overlaps more with the wagging peak, suggesting a greater role for these type of librations in the longitudinal phonon.

## G. Methanol & acetonitrile

To provide further evidence that the optical mode propagate along the H-bond network of water we decided to repeat our analysis for other polar liquids, both H-bonding and non-Hbonding. As an H-bonding liquid we choose methanol, which is known to contain winding H-bonded chains. According to results from MD simulation, most of these chains have around 5-6 molecules<sup>46,47</sup>, with a small percentage of chains containing 10-20 molecules.<sup>48</sup> Chain lifetimes have been estimated to be about .5 ps.<sup>48</sup> Therefore we expect methanol can also support a librational phonon mode that propagates along hydrogen bonds, but perhaps with a shorter lifetime and range than water. As a non H-bonding polar liquid we choose acetonitrile, because it has a structure similar to methanol, but with the hydroxyl group replaced by a carbon atom. We find that the OH librational band of methanol ( $\approx 700$  cm<sup>-1</sup>)<sup>49</sup> is indeed dispersive (see Supplementary Figure 5). As with water, the transverse spectra also exhibits dispersion, but to a much lesser extent. LO-TO splitting of about 100 cm<sup>-1</sup> is observed in the 700 cm<sup>-1</sup> librational peak. The results for acetonitrile are more ambiguous - we observe dispersion in the broad peak at  $\approx 100$  cm<sup>-1</sup>, however this peak contains contributions from translational and (free) rotational modes, as well as the CH<sub>3</sub> torsion mode, and it is not clear which modes are responsible for the dispersion (see Supplementary Figure 6).

| Model              | Temp | $\omega_{LO}$ | $\tau_{LO}$ | $\omega_{TO}$ | $\tau_{TO}$ | $\omega_{LO} - \omega_{TO}$ |
|--------------------|------|---------------|-------------|---------------|-------------|-----------------------------|
| TIP4P/2005f        | 250  | 905           | .38         | 667           | .23         | 233                         |
|                    | 300  | 900           | .44         | 632           | .18         | 268                         |
|                    | 350  | 871           | .34         | 574           | .18         | 297                         |
|                    | 400  | 826           | .25         | 423           | .17         | 400                         |
| TTM3F              | 250  | 757           | .49         | 496           |             | 261                         |
|                    | 300  | 721           | .44         | 410           |             | 311                         |
|                    | 350  | 710           | .20         | 380           |             | 330                         |
| expt <sup>89</sup> | 253  | 820           |             | 641           |             | 179                         |
|                    | 300  | 759           |             | 556           |             | 203                         |

TABLE I: **Resonance frequencies (cm<sup>-1</sup>) and lifetimes (ps) for the propagating modes.** The values from simulation were computed at the smallest  $k$  in the system. The experimental values are approximate, based on the position of the max of the band.

## II. DISCUSSION

In this work we have presented several lines of evidence for optical phonons that propagate along the H-bond network of water. The longitudinal and transverse nonlocal susceptibility exhibit dispersive peaks with dispersion relations resembling optical phonons. As the temperature is lowered, the resonance frequencies and LO-TO splittings of these modes converge towards the values for phonons in ice Ih. By comparing our results with a recent study of ice XI we believe both optical phonon modes likely consist of coupled wagging and rocking librations.<sup>4041</sup>

This work fundamentally changes our understanding of the librational band in the Raman spectra of water by assigning the lower and higher frequency peaks to transverse and longitudinal optical modes. Our analysis of the self-distinct cancellation indicates that the middle Raman peak ( $\approx 600$  cm<sup>-1</sup>) belongs to the remnant of the single molecule wagging response which remains after the cancellation. Similarly, we are also led to a new interpretation the librational region of real part of the dielectric function. In the case of a lossless optical phonon the transverse phonon occurs where  $\varepsilon'(\omega) = \infty$  while the longitudinal phonon occurs where  $\varepsilon'(\omega) = 0$ . The presence of dampening moves smooths the divergence leading to a peak followed by a sharp dip. This is what is observed in the real part of the dielectric function of water between 300 - 500 cm<sup>-1</sup> (the features are shifted to lower frequencies by the tail of the low frequency Debye relaxation).

The large spatial range of these modes is surprising and studies with larger simulation boxes are needed to fully quantify their extent. The ability of water to transmit phonon modes may be relevant to biophysics, where they could lead to dynamical coupling between biomolecules, a phenomena which is currently only being considered at much lower frequencies.<sup>50-53</sup> The methodology used in this paper to analyse LO-TO splitting opens up a new

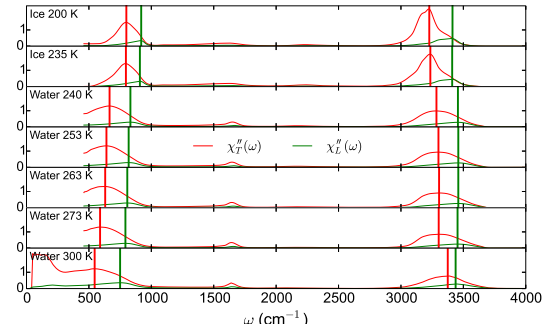


FIG. 8: **Static dielectric susceptibilities of ice and water.** Computed from index of refraction data using equations 1-3. data from 210 to 280 K comes from aerosol droplets<sup>8</sup> while the data at 300 comes from bulk liquid.<sup>9</sup>

avenue to understanding the structure and dynamics of water. The fact that the librational LO-TO splitting increases with temperature instead of the expected decrease is likely due to significant changes in the structure of the liquid. One likely possibility is that the volume per “unit cell” term in equation 6 decreases with temperature. This could be caused by the local quasi structure determined by H-bonding changing from a more ice-like structure (4 molecules per unit cell) to a more cubic structure (1 molecule per unit cell). More research is needed to understand the microscopic origin of the LO-TO splitting in water, both in the librational and stretching modes.

## III. METHODS

### A. Theory of the nonlocal susceptibility

If the external field is sufficiently small, the relation between the polarization response of a medium and the electric displacement field  $\mathbf{D}$  for a spatially homogeneous system is given by :

$$\mathbf{P}(\mathbf{r}, t) = \epsilon_0 \int_V \int_{-\infty}^t d\mathbf{r}' dt' \overleftrightarrow{\chi}(\mathbf{r} - \mathbf{r}', t - t') \mathbf{D}(\mathbf{r}', t') \quad (9)$$

This expression Fourier transforms to:

$$\mathbf{P}(\mathbf{k}, \omega) = \epsilon_0 \overleftrightarrow{\chi}(\mathbf{k}, \omega) \mathbf{D}(\mathbf{k}, \omega) \quad (10)$$

For isotropic systems, the tensor  $\overleftrightarrow{\chi}$  can be decomposed into longitudinal and transverse components:

$$\overleftrightarrow{\chi}(\mathbf{k}, \omega) = \chi_L(k, \omega) \hat{\mathbf{k}} \hat{\mathbf{k}} + \chi_T(k, \omega) (\mathbf{I} - \hat{\mathbf{k}} \hat{\mathbf{k}}) \quad (11)$$

The easiest starting point for deriving microscopic expressions for  $\chi_L(k, \omega)$  and  $\chi_T(k, \omega)$  is the classical Kubo

formula:<sup>54</sup>

$$\chi_{L/T}(\mathbf{k}, \omega) = \frac{\beta}{\epsilon_0} \int_0^\infty dt \frac{d}{dt} \langle \mathbf{P}_{L/T}(\mathbf{k}, t) \cdot \mathbf{P}_{L/T}^*(\mathbf{k}, 0) \rangle e^{i\omega t} \quad (12)$$

This expression relates the susceptibility to the time correlation function of the polarization in equilibrium. The longitudinal part of the polarization can be calculated by Fourier transforming the defining expression for the polarization  $\nabla \cdot \mathbf{P}(\mathbf{r}, t) = -\rho(\mathbf{r}, t)$ , leading to  $\hat{\mathbf{k}} \cdot \mathbf{P} = i\rho(\mathbf{k}, t)/k = P_L$ . To calculate the transverse part of the polarization we use the method of Raineri & Friedman to find the polarization vector of each molecule.<sup>55</sup> For ease of comparison and analysis, we define normalized polarization time correlation functions:

$$\Phi_{L/T}(\mathbf{k}, t) \equiv \frac{\langle \mathbf{P}_{L/T}(\mathbf{k}, t) \cdot \mathbf{P}_{L/T}^*(\mathbf{k}, 0) \rangle}{\langle \mathbf{P}_{L/T}(\mathbf{k}, 0) \cdot \mathbf{P}_{L/T}^*(\mathbf{k}, 0) \rangle} \quad (13)$$

Substituting this into equation 12 and taking into account the isotropy of water we obtain:

$$\chi_{L/T}(k, \omega) = \chi_{L/T}(k, 0) \int_0^\infty \dot{\Phi}_{L/T}(k, t) e^{i\omega t} dt \quad (14)$$

## B. Computational methods

The three water models we used were TIP4P/ $\epsilon$ ,<sup>56</sup> TIP4P/2005f,<sup>57</sup> and TTM3F.<sup>58</sup> To simulate methanol and acetonitrile we used the General AMBER Forcefield (GAFF),<sup>59</sup> a forcefield with full intramolecular flexibility which has been shown to satisfactorily reproduce key properties of both liquids.<sup>60</sup> Our TTM3F simulations were performed with an in-house code that uses the TTM3F force calculation routine of Fanourgakis and Xantheas. All other simulations were ran using the GROMACS package (ver. 4.6.5).<sup>61</sup> We used particle-mesh Ewald summation for the long range electrostatics with a Coulomb cutoff of 2 nm for our 4+ nm simulations and a cutoff of 1.2 nm for our simulations with 512 molecules. Our TTM3F simulations had 256 molecules and used Ewald summation and a Coulomb cutoff of .9 nm. The principle TIP4P/2005f simulations contained 512 molecules and were 8 ns long ( $\Delta t_{\text{out}} = 8$  fs) and .6 - 1.2 ns long ( $\Delta t_{\text{out}} = 4$  fs). Our TTM3F simulations were 1-2 ns long ( $\Delta t_{\text{out}} = 4$  fs). Simulations with MeOH and ACN contained 1,000 molecules and were 1 ns long ( $\Delta t_{\text{out}} = 8$  fs). All simulations were equilibrated for at least 50 ps prior to outputting data. The combination of long runs, a small output step and large boxes requires a lot of disk space, so we utilized the .xtc compression feature of GROMACS. Because of periodic boundary conditions, the possible  $\mathbf{k}$  vectors are limited to the form  $\mathbf{k} = 2\pi n_x \hat{\mathbf{i}}/L_x + 2\pi n_y \hat{\mathbf{j}}/L_y + 2\pi n_z \hat{\mathbf{k}}/L_z$ , where  $n_x, n_y$ , and  $n_z$  are integers. We calculated correlation functions separately for each  $\mathbf{k}$  and then average over the results for  $\mathbf{k}$  vectors with the same magnitude, a process we found greatly reduced random noise.

One can question whether a purely classical treatment is justified here because the librational dynamics we are interested have frequencies of 700-900 cm<sup>-1</sup> for which  $\hbar\omega \approx 3 - 4k_B T$  at 300 K. Previously it was shown that the widely-used harmonic approximation does not change the spectrum.<sup>11</sup> Furthermore, comparison of  $k$  resolved IR spectra taken from molecular dynamics and ab-initio DFT simulation show that they give qualitatively similar results for all frequencies below 800 cm<sup>-1</sup>.<sup>35</sup> For the OH stretching peak, however, quantum effects are known to be very important.

## C. Fitting the librational band

To obtain resonance frequencies and lifetimes for the librational peak in the imaginary part of the response we used a damped oscillator model. A Debye peak overlaps significantly with the librational band in both the longitudinal and transverse cases and must be included in the peak fitting. Equation 14 can be used to relate the form of the time correlation function to the absorption peak lineshape. For Debye response one has the following expressions:

$$\Phi(k, t) = Ae^{-t/\tau_D} \quad (15)$$

$$\frac{\text{Im}\{\chi(k, \omega)\}}{\chi(k, 0)} = \frac{A\omega\tau_D}{1 + \omega^2\tau_D^2}$$

For resonant response with resonance frequency  $\omega_0(k)$  and dampening factor  $\gamma \equiv 1/\tau$  we have:

$$\Phi(k, t) = Be^{-t/\tau} \cos(\omega_0 t) \quad (16)$$

$$\frac{\text{Im}\{\chi(k, \omega)\}}{\chi(k, 0)} = \frac{B}{2} \left( \frac{\omega\tau}{1 + (\omega + \omega_0)^2\tau^2} + \frac{\omega\tau}{1 + (\omega - \omega_0)^2\tau^2} \right)$$

We find this lineshape (the Van Vleck-Weisskopf lineshape<sup>62,63</sup>) yields results identical to the standard damped harmonic oscillator response for the range of  $\tau, \omega_0$  values we are interested in. We found a two function (Debye + resonant) fit worked very well for fitting the librational peak in the longitudinal case (see Supplementary Figures 7 and 8). The H-bond stretching peak at  $\approx 200$  cm<sup>-1</sup> overlaps with the librational band for  $2 < k < 2.5$ , and we found that it can be included in the fit using an additional damped harmonic oscillator, but usually this was not necessary. Because of this overlap and due to the broad nature of the transverse band, the fitting in the transverse case is only approximate. We found this was especially true for TTM3F and the experimental data, so we do not report lifetimes for such cases.

## IV. ACKNOWLEDGMENTS

This work was partially supported by DOE Award No. DE-FG02-09ER16052 (D.E) and by DOE Early Career Award No. de-sc0003871 (M.V.F.S.).

## REFERENCES

<sup>1</sup>Santra, B, Jr., R. A. D, Martelli, F, & Car, R. (in press 2015) Local structure analysis in ab initio liquid water. *Mol. Phys.* pp. 1–13.

<sup>2</sup>Errington, J. R & Debenedetti, P. G. (2001) Relationship between structural order and the anomalies of liquid water. *Nature* **409**, 318–321.

<sup>3</sup>English, N. J & Tse, J. S. (2011) Density fluctuations in liquid water. *Phys. Rev. Lett.* **106**, 037801.

<sup>4</sup>Huang, C, Wikfeldt, K. T, Tokushima, T, Nordlund, D, Harada, Y, Bergmann, U, Niebuhr, M, Weiss, T. M, Horikawa, Y, Leetmaa, M, Ljungberg, M. P, Takahashi, O, Lenz, A, Ojame, L, Lyubartsev, A. P, Shin, S, Pettersson, L. G. M, & Nilsson, A. (2009) The inhomogeneous structure of water at ambient conditions. *Proc. Natl. Acad. Sci. USA* **106**, 15214–15218.

<sup>5</sup>Sahle, C. J, Sternemann, C, Schmidt, C, Lehtola, S, Jahn, S, Simonelli, L, Huotari, S, Hakala, M, Pylkknen, T, Nyrow, A, Mende, K, Tolan, M, Hmlinen, K, & Wilke, M. (2013) Microscopic structure of water at elevated pressures and temperatures. *Proc. Natl. Acad. Sci. USA* **110**, 6301–6306.

<sup>6</sup>Madden, P & Kivelson, D. (2007) in *Adv. Chem. Phys.* (John Wiley & Sons, Inc.), p. 467.

<sup>7</sup>Hansen, J.-P & McDonald, I. R. (2006) in *Theory of Simple Liquids (Third Edition)*, eds. Hansen, J.-P & McDonald, I. R. (Academic Press), 3rd edition edition, p. 341.

<sup>8</sup>Zasetsky, A. Y, Khalizov, A. F, Earle, M. E, & Sloan, J. J. (2005) Frequency dependent complex refractive indices of supercooled liquid water and ice determined from aerosol extinction spectra. *The Journal of Physical Chemistry A* **109**, 2760.

<sup>9</sup>Hale, G & Querry, M. (1973) Optical constants of water in the 200-nm to 200- μm wavelength region. *Appl. Opt.* **12**, 555.

<sup>10</sup>Resat, H, Raineri, F. O, & Friedman, H. L. (1993) Studies of the optical like high frequency dispersion mode in liquid water. *J. Chem. Phys.* **98**, 7277.

<sup>11</sup>Bopp, P. A, Kornyshev, A. A, & Sutmann, G. (1998) Frequency and wave-vector dependent dielectric function of water: Collective modes and relaxation spectra. *J. Chem. Phys.* **109**, 1939.

<sup>12</sup>Walrafen, G. E. (1964) Raman spectral studies of water structure. *J. Phys. Chem.* **40**, 3249.

<sup>13</sup>Bolla, G. (1933) Su alcune nuove bande raman dell'acqua. *Il Nuovo Cimento* **10**, 101–107.

<sup>14</sup>Carey, D. M & Korenowski, G. M. (1998) Measurement of the raman spectrum of liquid water. *J. Chem. Phys.* **108**, 2669–2675.

<sup>15</sup>Walrafen, G. E. (1990) Raman spectrum of water: transverse and longitudinal acoustic modes below  $\approx 300 \text{ cm}^{-1}$  and optic modes above  $\approx 300 \text{ cm}^{-1}$ . *J. Phys. Chem.* **94**, 2237–2239.

<sup>16</sup>Walrafen, G. E. (1967) Raman spectral studies of the effects of temperature on water structure. *J. Phys. Chem.* **47**, 114–126.

<sup>17</sup>Walrafen, G. E, Fisher, M. R, Hokmabadi, M. S, & Yang, W. (1986) Temperature dependence of the low and highfrequency raman scattering from liquid water. *J. Chem. Phys.* **85**, 6970–6982.

<sup>18</sup>Castner, E. W, Chang, Y. J, Chu, Y. C, & Walrafen, G. E. (1995) The intermolecular dynamics of liquid water. *J. Chem. Phys.* **102**, 653–659.

<sup>19</sup>Zelmann, H. R. (1995) Temperature dependence of the optical constants for liquid h<sub>2</sub>o and d<sub>2</sub>o in the far ir region. *J. Mol. Str.* **350**, 95 – 114.

<sup>20</sup>Fukasawa, T, Sato, T, Watanabe, J, Hama, Y, Kunz, W, & Buchner, R. (2005) Relation between dielectric and low-frequency raman spectra of hydrogen-bond liquids. *Phys. Rev. Lett.* **95**, 197802.

<sup>21</sup>Aure, P & Chosson, A. (1978) The translational lattice-vibration raman spectrum of single crystal ice 1h. *J. Glaciology* **21**, 65–71.

<sup>22</sup>Klug, D. D, Tse, J. S, & Whalley, E. (1991) The longitudinaloptictransverseoptic mode splitting in ice 1h. *J. Chem. Phys.* **95**, 7011–7012.

<sup>23</sup>Whalley, E. (1977) A detailed assignment of the oh stretching bands of ice i. *Canadian Journal of Chemistry* **55**, 3429–3441.

<sup>24</sup>Klug, D. D & Whalley, E. (1978) Origin of the high-frequency translational bands of ice i\*. *J. Glaciology* **21**, 55–63.

<sup>25</sup>Galeener, F. L & Lucovsky, G. (1976) Longitudinal optical vibrations in glasses: Ge<sub>2</sub> and SiO<sub>2</sub>. *Phys. Rev. Lett.* **37**, 1474–1478.

<sup>26</sup>Lyddane, R. H, Sachs, R. G, & Teller, E. (1941) On the polar vibrations of alkali halides. *Phys. Rev.* **59**, 673–676.

<sup>27</sup>Barker, A. S. (1975) Long-wavelength soft modes, central peaks, and the lyddane-sachs-teller relation. *Phys. Rev. B* **12**, 4071–4084.

<sup>28</sup>Sievers, A. J & Page, J. B. (1990) Generalized lyddane-sachs-teller relation and disordered solids. *Phys. Rev. B* **41**, 3455–3459.

<sup>29</sup>Payne, M & Inkson, J. (1984) Longitudinal-optic-transverse-optic vibrational mode splittings in tetrahedral network glasses. *Journal of Non-Crystalline Solids* **68**, 351 – 360.

<sup>30</sup>Sekimoto, K & Matsubara, T. (1982) To-to splittings of glassy dielectrics. *Phys. Rev. B* **26**, 3411.

<sup>31</sup>Decius, J. C & Hexter, R. M. (1977) *Molecular Vibrations in Crystals*. (McGraw-Hill, USA).

<sup>32</sup>Decius, J. C. (1968) Dipolar coupling and molecular vibration in crystals. i. general theory. *J. Chem. Phys.* **49**, 1387–1392.

<sup>33</sup>Burba, C. M & Frech, R. (2011) Existence of optical phonons in the room temperature ionic liquid 1-ethyl-3-methylimidazolium trifluoromethanesulfonate. *J. Chem. Phys.* **134**, 134503.

<sup>34</sup>Elton, D. C & Fernández-Serra, M.-V. (2014) Polar nanoregions in water: A study of the dielectric properties of tip4p/2005, tip4p/2005f and ttm3f. *J. Chem. Phys.* **140**, 124504.

<sup>35</sup>Heyden, M, Sun, J, Forbert, H, Mathias, G, Havenith, M, & Marx, D. (2012) Understanding the origins of dipolar couplings and correlated motion in the vibrational spectrum of water. *J. Phys. Chem. Lett.* **3**, 2135–2140.

<sup>36</sup>Woodward, L. (1972) *Introduction to the theory of molecular vibrations and vibrational spectroscopy*. (Clarendon Press).

<sup>37</sup>Wagner, R, Benz, S, Mhler, O, Saathoff, H, Schnaiter, M, & Schurath, U. (2005) Mid-infrared extinction spectra and optical constants of supercooled water droplets. *J. Phys. Chem. A* **109**, 7099–7112.

<sup>38</sup>Vinh, N. Q, Sherwin, M. S, Allen, S. J, George, D. K, Rahmani, A. J, & Plaxco, K. W. (2015) High-precision gigahertz-to-terahertz spectroscopy of aqueous salt solutions as a probe of the femtosecond-to-picosecond dynamics of liquid water. *J. Chem. Phys.* **142**.

<sup>39</sup>Ellison, W. J. (2007) Permittivity of pure water, at standard atmospheric pressure, over the frequency range 025thz and the temperature range 0100c. *J. Phys. Chem. Ref. D at.* **36**, 1–18.

<sup>40</sup>Iwano, K, Yokoo, T, Oguro, M, & Ikeda, S. (2010) Propagating librations in ice xi: Model analysis and coherent inelastic neutron scattering experiment. *Journal of the Physical Society of Japan* **79**, 063601.

<sup>41</sup>Shigenari, T & Abe, K. (2012) Vibrational modes of hydrogens in the proton ordered phase xi of ice: Raman spectra above 400 cm1. *J. Chem. Phys.* **136**.

<sup>42</sup>Wan, Q, Spanu, L, Galli, G. A, & Gygi, F. (2013) Raman spectra of liquid water from ab initio molecular dynamics: Vibrational signatures of charge fluctuations in the hydrogen bond network. *Journal of Chemical Theory and Computation* **9**, 4124–4130.

<sup>43</sup>Lobo, R, Robinson, J. E, & Rodriguez, S. (1973) High frequency dielectric response of dipolar liquids. *J. Chem. Phys.* **59**, 5992–6008.

<sup>44</sup>Pollock, E. L & Alder, B. J. (1981) Frequency-dependent dielectric response in polar liquids. *Phys. Rev. Lett.* **46**, 950–953.

<sup>45</sup>Chandra, A & Bagchi, B. (1990) Collective excitations in a dense dipolar liquid: How important are dipolarons in the polarization relaxation of common dipolar liquids? *J. Chem. Phys.* **92**, 6833.

<sup>46</sup>Haughney, M, Ferrario, M, & McDonald, I. R. (1987) Molecular-dynamics simulation of liquid methanol. *The Journal of Physical Chemistry* **91**, 4934–4940.

<sup>47</sup>Yamaguchi, T, Benmore, C. J, & Soper, A. K. (2000) The structure of subcritical and supercritical methanol by neutron diffract-

tion, empirical potential structure refinement, and spherical harmonic analysis. *J. Chem. Phys.* **112**, 8976–8987.

<sup>48</sup>Matsumoto, M & Gubbins, K. E. (1990) Hydrogen bonding in liquid methanol. *J. Chem. Phys.* **93**, 1981–1994.

<sup>49</sup>Crowder, G. A & Cook, B. R. (1967) Acetonitrile: far-infrared spectra and chemical thermodynamic properties. discussion of an entropy discrepancy. *The Journal of Physical Chemistry* **71**, 914–916.

<sup>50</sup>Conti Nibali, V & Havenith, M. (2014) New insights into the role of water in biological function: Studying solvated biomolecules using terahertz absorption spectroscopy in conjunction with molecular dynamics simulations. *J. Am. Chem. Soc.* **136**, 12800.

<sup>51</sup>Ebbinghaus, S, Kim, S. J, Heyden, M, Yu, X, Heugen, U, Gruebele, M, Leitner, D. M, & Havenith, M. (2007) An extended dynamical hydration shell around proteins. *Proc. Natl. Acad. Sci. USA* **104**, 20749.

<sup>52</sup>Heyden, M & Havenith, M. (2010) Combining thz spectroscopy and md simulations to study protein-hydration coupling. *Methods* **52**, 74.

<sup>53</sup>Kim, S, Born, B, Havenith, M, & Gruebele, M. (2008) Real-time detection of proteinwater dynamics upon protein folding by terahertz absorption spectroscopy. *Angewandte Chemie International Edition* **47**, 6486.

<sup>54</sup>Kubo, R. (1957) Statistical-mechanical theory of irreversible processes. i. general theory and simple applications to magnetic and conduction problems. *J. Phys. Soc. Jap.* **12**, 570–586.

<sup>55</sup>Raineri, F. O & Friedman, H. L. (1993) Static transverse dielectric function of model molecular fluids. *J. Chem. Phys.* **98**.

<sup>56</sup>Fuentes-Azcatl, R & Alejandre, J. (2014) Non-polarizable force field of water based on the dielectric constant: Tip4p/ $\varepsilon$ . *J. Phys. Chem. B* **118**, 1263–1272.

<sup>57</sup>Gonzalez, M. A & Abascal, J. L. F. (2011) A flexible model for water based on tip4p/2005. *J. Chem. Phys.* **135**, 224516.

<sup>58</sup>Fanourgakis, G. S & Xantheas, S. S. (2008) Development of transferable interaction potentials for water. v. extension of the flexible, polarizable, thole-type model potential (ttm3-f, v. 3.0) to describe the vibrational spectra of water clusters and liquid water. *J. Chem. Phys.* **128**, 074506.

<sup>59</sup>Wang, J, Wolf, R. M, Caldwell, J. W, Kollman, P. A, V, T, Wang, J, & Words, K. (2004) Development and testing of a general amber force field. *J. Compt. Chem.* **25**, 1157.

<sup>60</sup>Caleman, C, van Maaren, P. J, Hong, M, Hub, J. S, Costa, L. T, & van der Spoel, D. (2012) Force field benchmark of organic liquids: Density, enthalpy of vaporization, heat capacities, surface tension, isothermal compressibility, volumetric expansion coefficient, and dielectric constant. *J. Chem. Theo. Comp.* **8**, 61.

<sup>61</sup>Hess, B, Kutzner, C, van der Spoel, D, & Lindahl, E. (2008) Gromacs 4: Algorithms for highly efficient, load-balanced, and scalable molecular simulation. *J Chem. Theo. Comp.* **4**, 435–447.

<sup>62</sup>Toda, M, Kubo, R, Saitō, N, & Hashitsume, N. (1991) *Statistical Phys. II: Nonequilibrium Statistical Mechanics*, Series C, English Authors. (Springer Berlin Heidelberg).

<sup>63</sup>Van Vleck, J. H & Weisskopf, V. F. (1945) On the shape of collision-broadened lines. *Rev. Mod. Phys.* **17**, 227–236.

<sup>64</sup>Walrafen, G. E. (1962) Raman spectral studies of the effects of electrolytes on water. *J. Chem. Phys.* **36**, 1035–1042.

<sup>65</sup>Buchner, R, Barthel, J, & Stauber, J. (1999) The dielectric relaxation of water between 0c and 35c. *Chem. Phys. Lett.* **306**, 57.

<sup>66</sup>Bagchi, B & Chandra, A. (1993) Molecular theory of under-damped dielectric relaxation: understanding collective effects in dipolar liquids. *Chem. Phys.* **173**, 133 – 141.

<sup>67</sup>Ferraro, R & Basile, L. (1978) *Fourier Transform Infrared Spectra: Applications to Chem. Systems*. (Elsevier Science) Vol. v. 1.

<sup>68</sup>Bagchi, B & Chandra, A. (1992) Ultrafast solvation dynamics: Molecular explanation of computer simulation results in a simple dipolar solvent. *J. Chem. Phys.* **97**.

<sup>69</sup>Hill, N. E. (1971) The influence of the poley absorption on the inertial fall-off of the dielectric absorption. *J. Phys. C: Solid State Phys.* **4**, 2322.

<sup>70</sup>Nora E. Hill, W. E. Vaughan, A. P. M. D. (1963) *Dielectric Properties and Molecular Behaviour*. (Van Norstrand Reinhold Company, New York).

<sup>71</sup>Poley, J. (1955) Microwave dispersion of some polar liquids. *App. Sci. Res. B* **4**, 337–387.

<sup>72</sup>Kivelson, D & Friedman, H. (1989) Longitudinal dielectric relaxation. *J. Phys. Chem.* **93**, 7026–7031.

<sup>73</sup>Heyden, M, Sun, J, Funkner, S, Mathias, G, Forbert, H, Havenith, M, & Marx, D. (2010) Dissecting the thz spectrum of liquid water from first principles via correlations in time and space. *Proc. Natl. Acad. Sci. USA* **107**, 12068–12073.

<sup>74</sup>Bertolini, D & Tani, A. (1992) The frequency and wavelength dependent dielectric permittivity of water. *Mol. Phys.* **75**, 1065–1088.

<sup>75</sup>Lobo, R, Rodriguez, S, & Robinson, J. E. (1967) Collective excitations of dipolar systems. *Phys. Rev.* **161**, 513–525.

<sup>76</sup>Omelyan, I. P. (1996) Wavevector- and frequency-dependent dielectric constant of the stockmayer fluid. *Mol. Phys.* **87**, 1273–1283.

<sup>77</sup>Nee, T & Zwanzig, R. (1970) Theory of dielectric relaxation in polar liquids. *J. Chem. Phys.* **52**, 6353–6363.

<sup>78</sup>Fatuzzo, E & Mason, P. R. (1967) A calculation of the complex dielectric constant of a polar liquid by the librating molecule method. *Proc. Phys. Soc.* **90**, 729.

<sup>79</sup>Buchner, R, Barthel, J, & Stauber, J. (1976) Collective modes in dipolar liquids detection of dipolar plasmons. *Chem. Phys. Lett.* **39**, 23.

<sup>80</sup>Gerschel, A, Grochulski, T, Kisiel, Z, Pszczolkowski, L, & Leibler, K. (1985) High frequency rotational mode in liquid methyl chloride. *Mol. Phys.* **54**, 97–117.

<sup>81</sup>Afsar, M, Chantry, G, Birch, J, & Kilp, H. (1978) Far-infrared reflection measurements on nitromethane and the relevance of the plasmon model. *Infr. Phys.* **18**, 843 – 848.

<sup>82</sup>Bagchi, B & Chandra, A. (2009) *Collective Orientational Relaxation in Dense Dipolar Liquids*, Adv. Chem. Phys. (Wiley) No. 80, p. 1.

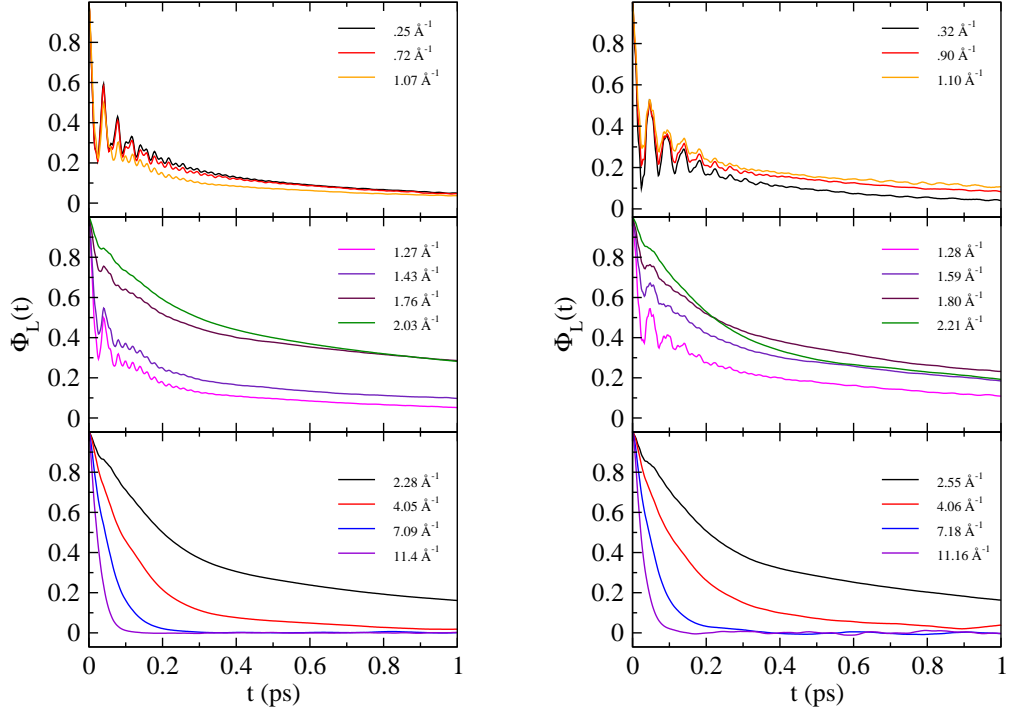
<sup>83</sup>Sedlmeier, F, Shadkhoo, S, Bruinsma, R, & Netz, R. R. (2014) Charge/mass dynamic structure factors of water and applications to dielectric friction and electroacoustic conversion. *J. Chem. Phys.* **140**.

## V. SUPPLEMENTARY INFORMATION

| type       | $\omega_{L1}$ | $\omega_{L2}$ | $\omega_{L3}$ | ref.                                   |
|------------|---------------|---------------|---------------|--|
| Raman      | 510           | —             | 780           | Bolla (1933) <sup>13</sup>             |
|            | 450           | —             | 780           | Walrafen (1962) <sup>64</sup>          |
|            | 400           | —             | 700           | Fukasawa, et. al. (2005) <sup>20</sup> |
|            | 430           | 650           | 795           | Carey, et. al. (1998) <sup>14</sup>    |
|            | 440           | 540           | 770           | Castner, et. al. (1995) <sup>18</sup>  |
|            | 450           | 550           | 725           | Walrafen (1990) <sup>15</sup>          |
|            | 424           | 550           | 725           | Walrafen (1986) <sup>17</sup>          |
|            | 439           | 538           | 717           | Walrafen (1967) <sup>16</sup>          |
| infrared   | 380           | 665           | —             | Zelmann (1995) <sup>19</sup>           |
| dielectric | 420           | 620           | —             | Fukasawa, et. la. (2005) <sup>20</sup> |

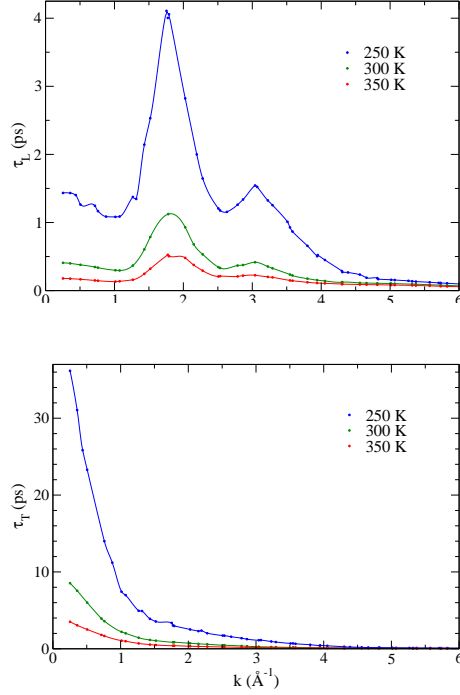
**Supplementary Table I: Experimental Raman, dielectric, and IR spectra giving 2 peak and 3 peak fits to the librational region at 298 K.**

## VI. POLARIZATION RELAXATION FUNCTIONS

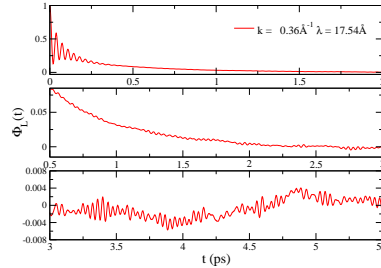


**Supplementary Figure 1: Longitudinal polarization relaxation functions.** Shown for 512 TIP4P2005/f (left) and TTM3F (right) at 300 K.

Relaxation times can be computed by fitting exponentials to the correlation functions. Figure 2 shows the longitudinal and transverse relaxation times of TIP4P/2005f at 300 K. We see that the longitudinal relaxation exhibits a peak at  $k \approx 2\text{\AA}^{-1}$ ,  $\lambda = 2.1\text{\AA}$  and a secondary peak at  $k \approx 3\text{\AA}^{-1}$ ,  $\lambda \approx 3.1\text{\AA}$ . The first peak is close to  $k$  values corresponding to the O-H distance in the hydrogen bond, while the second is close to the O-O distance.

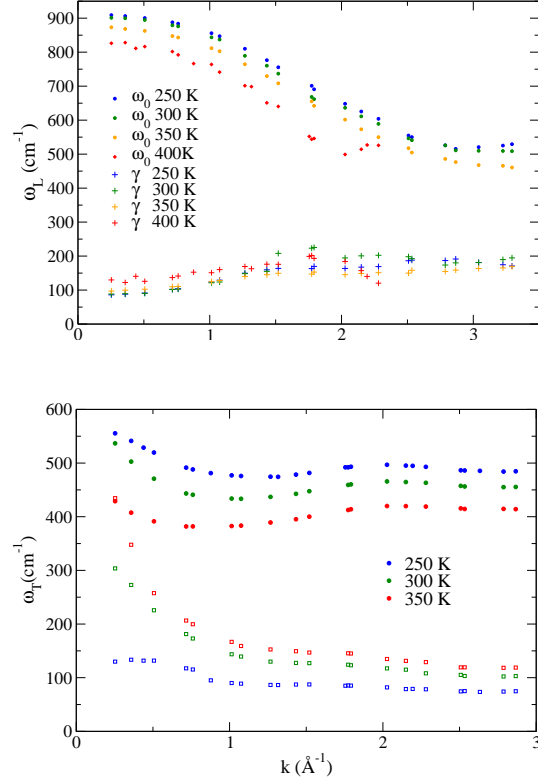


**Supplementary Figure 2: Longitudinal (top) and transverse (bottom) relaxation times for 512 TIP4P/2005f.** Computed for the underlying exponential of the relaxation. The points are interpolated by Akima splines. The transverse relaxation time here is equal to the Debye relaxation time, which at  $k = 0$  is  $\approx 11$  ps at 300 K. Experimentally it is 8.5 ps.<sup>65</sup>



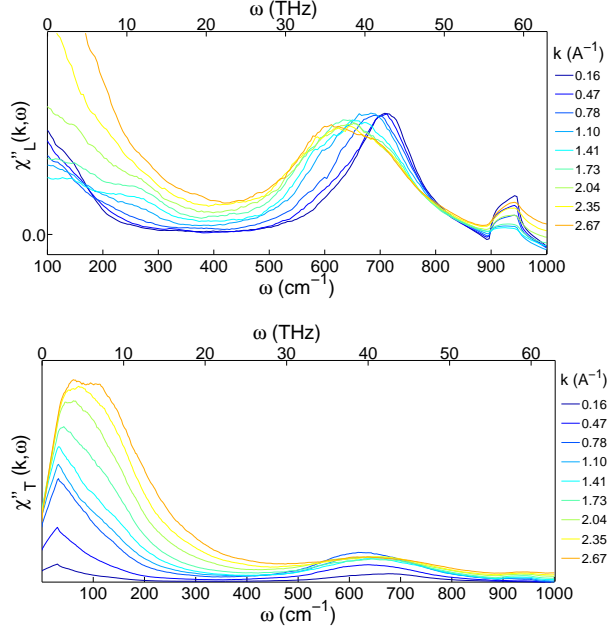
**Supplementary Figure 3: Fine features of the longitudinal polarization correlation function for 512 TIP4P/ε at 300 K.** Coherent small-magnitude oscillations appear to persist for longer than 1 ps.

#### A. Dispersion relations and dampening factors

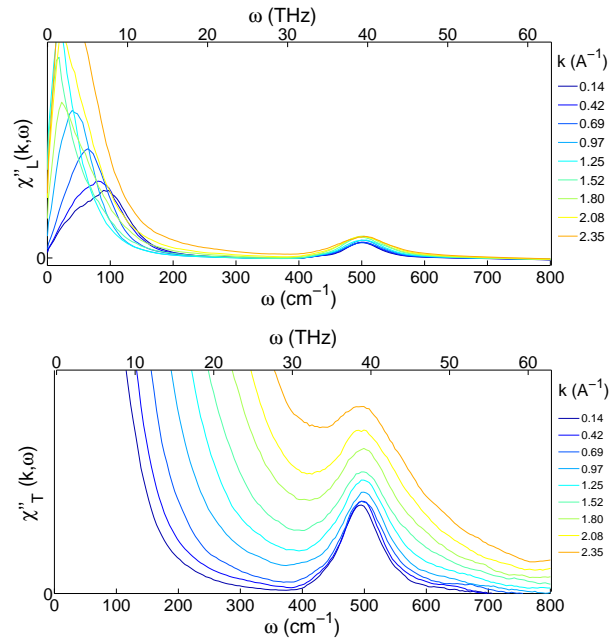


**Supplementary Figure 4: Longitudinal (top) and transverse (bottom) dispersion relations (circles) and dampening factors (squares) for 512 TIP4P/2005f.** These curves were obtained from a two peak (Debye + resonant) fit. In contrast to the longitudinal mode, the transverse mode is much more damped. However, the dampening factor changes significantly with temperature, also in contrast to the longitudinal case, and at 250 K becomes relatively small. Beyond  $2 \text{ \AA}^{-1}$  the peak due to the damped resonance starts to disappear so values beyond  $3 \text{ \AA}^{-1}$  are not shown.

## VII. METHANOL & ACETONITRILE

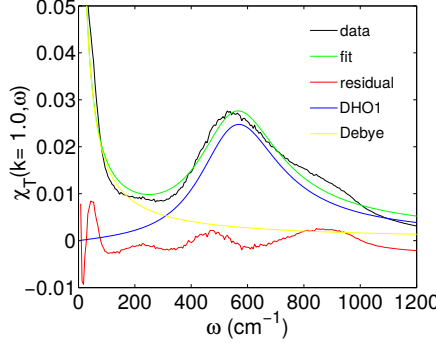


**Supplementary Figure 5: Longitudinal (top) and transverse (bottom) dielectric susceptibility for a system of 1,000 MeOH molecules.** The longitudinal librational peak at  $\approx 700 \text{ cm}^{-1}$  clearly disperses with  $k$ , while the transverse peak at  $\approx 600 \text{ cm}^{-1}$  disperses slightly with  $k$ . The higher frequency peaks exhibit no dispersion. The static dielectric function  $\varepsilon(k, 0)$  has not converged properly in the transverse case, so the magnitude of the peaks is not converged.

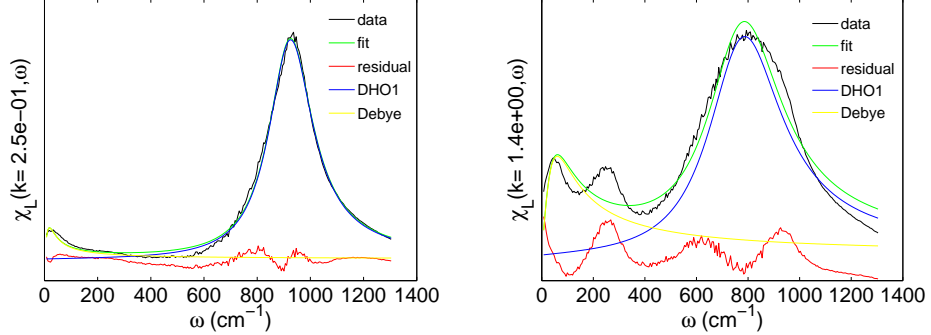


**Supplementary Figure 6: Longitudinal (top) and transverse (bottom) dielectric susceptibility for a system of 1,000 acetonitrile molecules.** The broad band which peaks at  $100 \text{ cm}^{-1}$  exhibits dispersion. We hypothesize this dispersion is due entirely to the translational modes, however we cannot say for sure since the librational and translational modes overlap in this region. The peak at  $\approx 500 \text{ cm}^{-1}$  is due to CCN bending. The static dielectric function  $\varepsilon(k, 0)$  has not converged properly, so the magnitude of the transverse peaks is not converged correctly, but the position of the peaks and dispersion can be seen.

### A. Examples of fitting



**Supplementary Figure 7: Example of fitting the transverse susceptibility of TIP4P/2005f at 300 K.**  
Fit with a Debye function and one damped harmonic oscillator at  $k = .25\text{\AA}^{-1}$  and  $k = 1.4\text{\AA}^{-1}$ . The residual show the parts not captured by the fit.



**Supplementary Figure 8: Examples of fitting the longitudinal susceptibility of TIP4P/2005f at 300K.**  
Fit with a Debye function and one damped harmonic oscillator at  $k = .25\text{\AA}^{-1}$  (left) and  $k = 1.4\text{\AA}^{-1}$  (right). The residual show the parts not captured by the fit. Two peaks appear in the residual - the lower frequency peak is dispersive, having the same dispersion relation as the fitted peak, suggesting that it is actually part of the dispersive peak lineshape that is not captured by our lineshape function. The higher frequency peak in the residual is non-dispersive and is in the same location for both the transverse and longitudinal susceptibility.

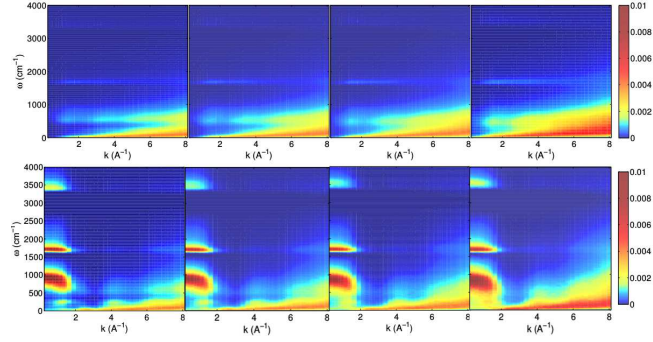
### B. Supplementary info: polarization-polarization structure factors

To assist in visualizing  $\chi_{L,T}(k, \omega)$  we introduce longitudinal and transverse “polarization-polarization structure factors:

$$S_{L,T}^{PP}(k, \omega) = \int_0^\infty \dot{\Phi}_{L,T}(k, t) e^{i\omega t} dt \quad (16)$$

Thus,  $\chi_{L,T}(k, \omega) = \chi_{L,T}(k, 0) S_{L,T}^{PP}(k, \omega)$ . These plots are shown solely because they provide a nice visual overview of the features in the nonlocal susceptibility. The main novel feature that appears in these plots is the low frequency acoustic-like mode originating at  $\approx 60 \text{ cm}^{-1}$ . This mode is purely intramolecular in nature and arises from inertial rotation.<sup>6667</sup> At very high wavenumbers ( $k > 7$ ) the relaxation is described by a rapidly decaying exponential and a Gaussian function.<sup>68</sup>

$$\Phi_L(k, t) = A(k) e^{t/\tau_1(k)} + B(k) e^{-(t/\tau_2(k))^2} \quad (17)$$



**Supplementary Figure 9:** Imaginary part of the longitudinal (top) and transverse (bottom) polar structure factor for TIP4P/2005f at 250 K, 300 K, 350 K, and 400 K (left to right). Note the increased intensity of the low frequency, high wavenumber intramolecular mode at higher temperatures. This is likely due to weaker H-bonding and greater freedom for inertial motion, which is responsible for this band.

Gaussian relaxation yields the following equation for the imaginary part of the susceptibility:

$$\begin{aligned} \Phi(k, t) &= Be^{-(t/\tau)^2} \\ \text{Im}\{\chi(k, \omega)\} &= \chi(k, 0)B \frac{\sqrt{\pi}}{2} \omega \tau^2 e^{-\frac{1}{4}\tau^2 \omega^2} \end{aligned} \quad (18)$$

The real part is:

$$\text{Re}\{\chi(k, \omega)\} = \chi(k, 0)B(\tau - \tau^2 \omega F(\omega \tau/2)) \quad (19)$$

where  $F()$  is Dawson's integral. The Gaussian form for the correlation function can be derived by considering a free rigid dipole subjected to Brownian kicks. In that case the relaxation function can be computed exactly.<sup>69</sup>

$$\phi(t) = \exp \left[ -\frac{t}{\tau_1} + \frac{\tau_2}{\tau_1} \left\{ 1 - \exp \left( -\frac{t}{\tau_2} \right) \right\} \right] \quad (20)$$

where  $\tau_1 = \xi/2k_B T$  and  $\tau_2 = I/\xi$  and  $\xi$  is the friction. In either the limit  $\xi \rightarrow 0$  or  $t \rightarrow 0$  one obtains the Gaussian form. Thus the interpretation of the Gaussian form is that it is due to fast inertial relaxation. It has been suggested that such inertial relaxation is origin of the Poley absorption that has been found in some dipolar liquids.<sup>69,70</sup> “Poley absorption” appears to be used as a general term for absorption of unknown origin found in many polar liquids around  $10 \text{ cm}^{-1}$  (.3 THz),<sup>70</sup> first described by Poley in 1955.<sup>71</sup> It has been variously described as being due to fast inertial “rattling” of molecules within their potential energy basins or as due to fast librational/inertial motion analogous to the rotational absorption of gas molecules.<sup>66,67</sup>

### VIII. APPLYING THE GLST RELATION TO WATER AT 300 K

For a dielectric function described by a single Debye relaxation, the LST relation is:<sup>27</sup>

$$\frac{\omega_L}{\omega_T} = \frac{\tau_T}{\tau_L} = \frac{\varepsilon(0)}{\varepsilon_\infty} \quad (21)$$

This equation can be derived on very general grounds from electromagnetic theory. As described by Kivelson, et. al. (1989) in general the longitudinal relaxation time in the long wavelength limit is smaller because of greater cancellation between the self and distinct terms.<sup>72</sup> In the case of TIP4P/2005f, for the smallest  $k$  in the 512 molecule system we find  $\tau_T/\tau_L = 8.7/.4 = 22$ . The dielectric constant is  $\approx 62$ , and in our previous work we estimated  $\varepsilon_\infty$  to be very close to 1, so the right hand side of the gLST relation is  $\approx 62$ .

If we add two damped harmonic oscillator modes we get the following gLST equation:

$$\frac{\tau_T}{\tau_L} \frac{(\omega_{1L}^2 + \gamma_{1L}^2)}{\omega_{1T}^2} \frac{(\omega_{2L}^2 + \gamma_{2L}^2)}{\omega_{2T}^2} = \frac{\varepsilon(0)}{\varepsilon_\infty} \quad (22)$$

For TIP4P/2005f,  $\frac{\omega_{1L}^2 + \gamma_{1L}^2}{\omega_{1T}^2} = 2.04$  for dispersive librational mode and  $\frac{\omega_{2L}^2 + \gamma_{2L}^2}{\omega_{2T}^2} \approx 1.06$  for the OH stretching band. This makes the left hand side of the gLST relation 44.6. A factor of 1.33 on the left hand side remains unaccounted for. Most likely this is due to LO-TO splitting in the H-bond stretching and bending modes, which have been shown to have LO-TO splitting in ice. The secondary and (controversial) tertiary Debye relaxation will contribute as well - LO-TO splitting in Debye relaxation is unavoidable, although its magnitude can be influenced by the presence of overlapping modes. Applying the gLST equation to water as a means of validating different fit functions in the low frequency region will be the subject of future work.

### IX. NOTES ON THE SPATIAL DECOMPOSITION OF SPECTRA

There are several different ways to “decompose” a spectra into contributions from molecules separated by distance  $R$ :

#### A. “Kirkwood” dipole-sphere method

This is the method we choose, which is a modification of the “sphere-sphere” method (see below). We start with the time-correlation function of interest :

$$\phi(t) = \left\langle \sum_i \boldsymbol{\mu}_i(0) \cdot \sum_j \boldsymbol{\mu}_j(t) \right\rangle \quad (23)$$

Here  $\boldsymbol{\mu}$  can be replaced with any dynamical variable of interest, for instance  $\mathbf{p}^T(\mathbf{k}, t)$  or  $\mathbf{j}(t)$ . We omit the  $k$  dependence for simplicity.

The most straightforward way is to limit the molecules around each molecule  $i$  to those in a sphere of radius  $R$ :

$$\phi(t, R) = \left\langle \sum_i \boldsymbol{\mu}_i(0) \cdot \sum_{j \in R_i} \boldsymbol{\mu}_j(t) \right\rangle \quad (24)$$

This is similar to the method employed by Bopp & Kornyshev. During the course of a simulation molecules enter and leave each sphere, which creates noise, requiring longer averaging times. This can be improved by utilizing a smooth cutoff function:

$$\phi(t, R) = \left\langle \sum_i \boldsymbol{\mu}_i(0) \cdot \sum_j P_{ij}(t) \boldsymbol{\mu}_j(t) \right\rangle \quad (25)$$

where

$$P_{ij} = \frac{1}{1 + e^{(R_{ij} - R)/D}} \quad (26)$$

Here  $D$  is a “sharpness parameter” determining the relative sharpness of the cutoff. We choose not to use smoothing however, finding it to be unnecessary. The result is a spectra  $\chi(\mathbf{k}, \omega, R)$  showing contributions from molecules up to radius  $R$ . The resulting function exhibits the expected  $R \rightarrow 0$  limit, yielding only the self contribution. In the  $R \rightarrow \infty$  limit, the original full response function is recovered. This function can then be numerically differentiated to show the contributions from shells of thickness  $\Delta R$  centered at distance  $R$ .

#### B. Sphere-sphere method

Another method discussed by Heyden, et. al. (2010) is to study the *autocorrelation* of the total dipole moment of a sphere of radius  $R$  centered around a reference molecule, and then average over each molecule in the system.<sup>73</sup>

$$\phi^P(t, R) = \sum_i \langle \boldsymbol{\mu}_i^P(0) \cdot \boldsymbol{\mu}_i^P(t) \rangle \quad (27)$$

where

$$\boldsymbol{\mu}_i^P(t) = \mathcal{N}_i(t) \sum_{j \in R_i} P_{ij}(t) \boldsymbol{\mu}_j(t) \quad (28)$$

Heyden, et. al. recommend the normalization factor  $\mathcal{N}_i(t) = (1 + \sum_{j \in R_i} P_{ij}^2)^{-1/2}$  to normalize for number of molecules in each sphere. This normalization factor is chosen so that in the bulk limit ( $R \rightarrow \infty$ ) the original full response function is obtained (in that limit  $\mathcal{N}_i = 1/\sqrt{N_{\text{mol}}}$ ). In the limit  $R \rightarrow 0$  only the self-term contributes. Results from this method must be interpreted with a bit of care since the calculation includes all

cross-correlations between molecules within the sphere centered around the reference molecule. We found that this method is more sensitive to intermolecular correlations, in particular the H-bond stretching at  $\approx 250 \text{ cm}^{-1}$  (not shown). Altogether though we found the results from this method are complementary with our results from the dipole-sphere method.

### C. Spatial grid method

To achieve higher resolution, Heyden, et. al. also introduce a spatial grid method.<sup>73</sup> The method works by binning the molecular dipoles into grid cells. To reduce noise caused by molecules moving in and out of bins the binning is Gaussian, meaning the dipoles are smeared with a Gaussian function. Unlike the other methods the spatial grid method does not yield the self part as  $R \rightarrow 0$  so this limit requires special interpretation.

## X. MULTIPOLAR EXPANSION OF INTRAMOLECULAR PART

The following section shows the relation of the polarization to the dipole moments of the molecules. We see that the representation of polarization as a sum of molecular dipole moments is only valid in the  $k \rightarrow 0$  limit. We start with the defining equation of the polarization  $\nabla \cdot \mathbf{P}(\mathbf{r}, t) = -\rho(\mathbf{r}, t)$  transformed in  $k$  space. The equation

$$\hat{\mathbf{k}} \cdot \mathbf{P} = \frac{i\rho(\mathbf{k}, t)}{k} = P_L \quad (29)$$

yields the following Kubo formula for the longitudinal part of the response:

$$\chi_L(\mathbf{k}, \omega) = \frac{\beta}{\epsilon_0 k^2} \int_0^\infty dt \frac{d}{dt} \langle \rho(\mathbf{k}, t) \rho^*(\mathbf{k}, 0) \rangle e^{i\omega t} \quad (30)$$

For a system composed of point charges, the charge density is :

$$\rho(\mathbf{r}, t) = \frac{1}{V} \sum_i \sum_\alpha q_{i\alpha} \delta(\mathbf{r} - \mathbf{r}_i(t) - \mathbf{r}_{i\alpha}(t)) \quad (31)$$

Here the index  $i$  runs over the molecules,  $\alpha$  runs over the atomic sites on each molecule,  $\mathbf{r}_i$  is the position of the center of mass of molecule  $i$  and  $\mathbf{r}_{i\alpha} = \mathbf{r}_i(t) - \mathbf{r}_\alpha(t)$ . The charge density in  $k$ -space becomes:

$$\rho(\mathbf{k}, t) = \frac{1}{V} \sum_i \sum_\alpha q_\alpha e^{-i\mathbf{k} \cdot (\mathbf{r}_i(t) + \mathbf{r}_{i\alpha}(t))} \quad (32)$$

Note that eqn. 32 can be Taylor expanded as:

$$\begin{aligned} \frac{\rho(\mathbf{k}, t)}{k} &= \frac{1}{k} \sum_i \sum_\alpha q_\alpha \sum_n \frac{(-i\mathbf{k} \cdot \mathbf{r}_{i\alpha}(t))^n}{n!} \\ &= \mathbf{M}(\mathbf{k}, t) + \mathbf{Q}(\mathbf{k}, t) + \mathbf{O}(\mathbf{k}, t) + \dots \end{aligned} \quad (33)$$

Here  $\mathbf{M}(\mathbf{k}, t)$ ,  $\mathbf{Q}(\mathbf{k}, t)$ ,  $\mathbf{O}(\mathbf{k}, t)$  are contributions due to the molecular dipoles, quadrupoles and octupoles. In the limit  $k \rightarrow 0$  it from eqn. 30 it can be seen that only the dipole term contributes to the susceptibility. One obtains

$$\chi_L(k, \omega) \approx \frac{\beta}{3\epsilon_0 V} \int_0^\infty dt \frac{d}{dt} \langle \mathbf{M}_L(\mathbf{k}, t) \cdot \mathbf{M}_L^*(\mathbf{k}, 0) \rangle e^{i\omega t} \quad (34)$$

with

$$\mathbf{M}_L(\mathbf{k}, t) = \sum_{i=1}^{N_{\text{mol}}} \hat{\mathbf{k}} \cdot \boldsymbol{\mu}_i(t) e^{i\mathbf{k} \cdot \mathbf{r}_i(t)} \quad (35)$$

This expression has been used previously as an approximate expression at small  $k$ .<sup>74</sup> However, Bopp & Kornyshev show quite convincingly that for water the higher order multipole terms are very important, even at the smallest  $k$  available in computer simulation.<sup>11</sup> Neglect of the higher order terms leads to severe consequences at large  $k$ , and one will not recover the physical limit  $\lim_{k \rightarrow \infty} \chi(k) = 1$  unless higher order terms are included.

### A. Supplementary info: Dipolar plasmon interpretation

A possible alternative to the optical phonon interpretation which we found warranted serious investigation is that the librational mode is a dipolar plasmon (also called, somewhat confusingly, a “dipoleon”). For systems of dipoles there is predicted to exist a dipolar plasmon modes analogous to the plasmon mode found in one component plasmas such as the free electron gas.<sup>4375</sup> Dipolar plasmons have been claimed to be observed in molecular dynamics simulation of point dipoles with the Lennard-Jones interaction (the “Stockmayer system”).<sup>4476</sup>

As far as we know the possibility that the librational peak in the dielectric susceptibility of water is a dipolar plasmon peak has not been considered in detail before. The dipolar plasmon corresponds to different physics than the optical phonon picture. The theory of the dipolar plasmon is based on the dielectric function derived by Nee & Zwanzig<sup>77</sup> and separately Fatuzzo & Mason<sup>78</sup> using a dynamical version of the Onsager cavity mean field model. The model they employ makes no mention of molecular interactions such as H-bonds, and instead consists of a single molecular dipole interacting with a cavity reaction field and undergoing random Brownian motion. To obtain the dipolar plasmon, the dielectric function is modified by including inertial effects and by making the Brownian friction exponentially correlated instead of delta correlated. The physics of the dipolar plasmon is easiest to understand by picturing a dipole undergoing small librations and being driven by an external plane wave electric field (this picture is the starting point of Fatuzzo & Mason). In equilibrium the reaction field always points in the same direction as the dipole, but if the dipole is rotating the reaction field will exhibit a phase

lag in time (whenever the imaginary part of the dielectric function is nonzero). The phase lagged reaction field acts to counter the rotation of the dipole, an effect called rotational dielectric friction. At high enough driving frequencies a resonance can be set up between the librating dipole and the phase-lagged reaction field response.

The clearest evidence we found that the dispersion we observed is due to a dipolar plasmon comes from comparing the nonlocal susceptibility we observe with the results for dipolar plasmon observed in the Stockmayer system.<sup>44</sup> The change in peak shape during dispersion is almost identical in both cases. The transverse dipolar plasmon mode observed in the Stockmayer system is heavily damped, also in agreement with our observations. The frequencies predicted by Lobo, et. al. for the dipolar plasmon resonances in water ( $\omega_L = 636 \text{ cm}^{-1}$ ,  $\omega_T = 407 \text{ cm}^{-1}$ ) are also in fairly good agreement with our findings for TTM3F and experiment. However, the frequencies predicted by dipolar plasmon theory shift significantly depending on the time constant  $\tau$  chosen for the exponentially-correlated Brownian friction. Curiously, the dipolar plasmon only appears when the Brownian friction is exponentially correlated (frequency dependent), and disappears when the friction becomes delta correlated ( $\tau \rightarrow 0$ ). There is no well-defined way to choose  $\tau$  and it is not clear whether the argument given by Lobo, et. al. for their choice of  $\tau$  (based on the hydrogen bond energy) makes sense. When there is no Debye relaxation dipolar plasmon theory predicts that the polarization time correlation function contains oscillations of around zero.<sup>4443</sup> Dipolar plasmon theory can easily be extended to include a Debye term, in which case the polarization time correlation functions consist of an oscillation superimposed on an exponential.

There is scant experimental evidence for dipolar plasmons in dipolar liquids. Experimental observations of a dipolar plasmon peak have been suggested for both nitromethane<sup>79</sup> and methyl chloride,<sup>80</sup> although the former result was questioned.<sup>81</sup> On the basis of a hydrodynamic theory, Bagchi and Chandra argue that whether a dipolar plasmon is present depends on the parameter  $B = \frac{k_B T}{ID_r^2}$ .<sup>4582</sup> Here  $I$  is the moment of inertia of the molecule and  $D_r$  is the rotational diffusion constant. They found that  $B$  must be less than 5 for dipolar plasmons to exist, implying that they are unlikely to exist in most dipolar liquids since the rotational diffusion constant required is much too fast. If we take  $D_r \approx 1/\tau_s$  ( $\tau_s$  being the relaxation time for a single molecular dipole) then we find  $B \approx 800$  for water. However, this result does not conclusively rule out the existence of a dipolar plasmon in water since the hydrodynamic theory they employ is of questionable applicability to an H-bonding liquid like water. Bagchi & Chandra also found that the dipolar plasmon is enhanced by a large dielectric constant and by coupling between translational and rotational polarization relaxation, which has recently been found to be significant in water.<sup>83</sup> In some ways, the dipolar plasmon is very similar to an optical phonon. As

with optical phonons, for the pure dipolar plasmon the longitudinal and transverse modes occur when  $\varepsilon(\omega) = 0$  and  $\varepsilon(\omega) = \infty$ . The dispersion observed by Pollock & Adler is qualitatively similar to that of a phonon. The *pure* dipolar plasmon obeys an LST relation given by<sup>43</sup>

$$\frac{\omega_L^2}{\omega_T^2} = \frac{\varepsilon(0)}{\varepsilon_\infty} \left( \frac{2\varepsilon(0)}{\varepsilon(0) + \varepsilon_\infty} \right) \quad (36)$$

which apart from the factor of  $2\varepsilon(0)/(\varepsilon(0) + \varepsilon_\infty)$  is identical to the LST relation for ionic crystals.

A few other qualitative observations suggest a dipolar plasmon:

- The mode contains contributions from very long range correlations. This is an assumption of dipolaron theory, which assumes a molecule (or equivalently a collection of molecules) is surrounded by a cavity and interacts with the cavity reaction field created by long range electrostatics.
- The temperature dependence of speed of propagation of the mode is very small. This is expected since the strength of H-bonds changes significantly with temperature.

However, a key property of the dipolar plasmon resonance is that it is simultaneously a resonance of both the single dipole motion and the collective motion.<sup>43</sup> *This is not borne out when we compare the self and full response.* The underlying assumptions of the dipolar plasmon theory are also very questionable. The Onsager cavity picture neglects H-bonding and is known to give mediocre predictions for the dielectric constant. As mentioned, dipolar plasmon theory also contains a free parameter,  $\tau$ , for which there is no rigorous justification. Small changes in  $\tau$  change the frequencies predicted by the theory significantly. The objections raised by Bagchi & Chandra also represent a serious theoretical difficulty.<sup>4582</sup> The fact that dipolarons have not been unambiguously detected in other dipolar liquids (despite some efforts) confirms the assertion of Bagchi & Chandra that the moments of inertia found in dipolar liquids are too large.

There is also the issue of whether a dipolar plasmon in real materials would be in any way distinct from a normal optical phonon mode. The idealized dipolar plasmon, occurring in a system of point dipoles, cannot exist in nature, unlike the plasmon, which can exist in the free electron gas in metals or in a bi-component plasma (systems of point charges). Any realization of the dipolar plasmon in real materials has to be due to the rotation of molecules, ie. the motion of nuclei. Such collective oscillations of nuclei are better characterized as phonon modes. Nevertheless, the dipolar plasmon theory does offer some physical insight into the librational dynamics of water since there is no doubt that water molecules feel a reaction field as they undergo hindered rotation. The effect of this reaction field (dielectric friction) appears to be small, however and the moment of inertia of water appears to be too high to allow for a dipolar plasmon.